jth

ORIGINAL ARTICLE

Nanobodies against factor XI apple 3 domain inhibit binding of factor IX and reveal a novel binding site for high molecular weight kininogen

Awital Bar Barroeta[1] | J. Arnoud Marquart[1] | Kamran Bakhtiari[1] | Alexander B. Meijer[1,2] | Rolf T. Urbanus[3] | Joost C. M. Meijers[1,4,5]

[1]Department of Molecular Hematology, Sanquin, Amsterdam, the Netherlands

[2]Department of Pharmaceutics, Utrecht Institute for Pharmaceutical Sciences (UIPS), Utrecht University, Utrecht, the Netherlands

[3]Center for Benign Haematology, Thrombosis and Haemostasis, Van Creveldkliniek, University Medical Center Utrecht, University Utrecht, Utrecht, the Netherlands

[4]Department of Experimental Vascular Medicine, Amsterdam UMC, University of Amsterdam, Amsterdam, the Netherlands

[5]Amsterdam Cardiovascular Sciences, Pulmonary Hypertension and Thrombosis, Amsterdam, the Netherlands

Correspondence
Joost C. M. Meijers, Department of Molecular Hematology, Sanquin, Plesmanlaan 125, 1066 CX Amsterdam, the Netherlands.
Email: j.meijers@sanquin.nl

Funding information
Landsteiner Foundation for Blood Transfusion Research, Grant/Award Number: 1702

Abstract

Background: Factor XI (FXI) is a promising target for novel anticoagulants because it shows a strong relation to thromboembolic diseases, while fulfilling a mostly supportive role in hemostasis. Anticoagulants targeting FXI could therefore reduce the risk for thrombosis, without increasing the chance of bleeding side effects.

Objectives: To generate nanobodies that can interfere with FXIa mediated activation of factor IX (FIX).

Methods: Nanobodies were selected for binding to the apple 3 domain of FXI and their effects on FXI and coagulation were measured in purified protein systems as well as in plasma-based coagulation assays. Additionally, the binding epitope of selected nanobodies was assessed by hydrogen–deuterium exchange mass spectrometry.

Results: We have identified five nanobodies that inhibit FIX activation by FXI by competing with the FIX binding site on FXI. Interestingly, a sixth nanobody was found to target a different binding epitope in the apple 3 domain, resulting in competition with the FXI–high molecular weight kininogen (HK) interaction.

Conclusions: We have characterized a nanobody targeting the FXI apple 3 domain that elucidates the binding orientation of HK on FXI. Moreover, we have produced five nanobodies that can inhibit the FXI–FIX interaction.

KEYWORDS
anticoagulants, factor XI, high molecular weight kininogen, hydrogen–deuterium exchange mass spectrometrynanobody

1 | INTRODUCTION

Over the last decade factor XI (FXI) has emerged as a promising target for the development of novel anticoagulation therapy.[1–5] While direct oral anticoagulants (DOACs) have a lower bleeding incidence than the vitamin K antagonists they have replaced, DOACs still show a risk for bleeding due to their interference with thrombin or factor Xa, which have a crucial role in hemostasis.[3,4,6–9] FXI deficiency only causes a mild bleeding disorder and has been found to protect against thrombotic events such as venous thrombosis and ischemic stroke.[10–14] Accordingly, higher levels of FXI are a risk factor for venous thrombosis[12,15] and stroke.[16] Thus, zymogen FXI or its activated form, FXIa, could serve as a target for safer drugs to treat thrombosis with less risk for bleeding.

Various new treatments based on targeting FXI are in development. These include the reduction of FXI synthesis in the liver by antisense oligonucleotides,[17,18] small molecules that inhibit FXIa activity by blocking the active site directly or through allosteric action,[19,20] anti-FXI aptamers,[21] and FXI(a)-targeting antibodies.[22–25] Three FXI-targeting antibodies (abelacimab, xisocimab 3G3, and osocimab) are either in the final stage of phase 2 or entering phase 3 clinical trials.[23–27]

While treatment with humanized antibodies seems promising, repeated administration of biopharmaceuticals has been known to induce adverse immune responses through the generation of anti-drug antibodies.[28,29] In most cases these have a negligible effect on the treatment. However, antidrug antibodies can adversely affect the pharmacokinetics and bioavailability of the drug, reducing the efficacy of the antibody and at worst causing complete neutralization of its function. Moreover, antidrug antibodies can provoke allergic reactions or even autoimmune responses.[28] We therefore propose the development of a nanobody targeting FXI, thought to have lower immunogenicity compared to antibodies.[30]

Nanobodies are the isolated heavy chain antibody variable (VHH) domains obtained from camelid heavy-chain antibodies.[31] These VHH domains are homologous to the VH domain of a conventional antibody, and contain three loops, so-called complementarity-determining regions (CDRs), that establish nanobody specificity.[32,33] Despite their small size they show a target specificity and affinity that is comparable to antibodies.[29–31,34,35] Moreover, nanobody size and their extended flexible structure of the CDR3 loop allows them to target antigenic sites that are generally not recognized by antibodies.[35] While their size also causes rapid renal clearance, this can be overcome by various protein modifications such as fusion to a human serum albumin-binding domain.[33,36] Additional favorable characteristics of nanobodies include low immunogenicity, high solubility, and good tissue penetration *in vivo*.[29–31,34,35] Last, nanobodies can be produced easily in bacteria and yeast whereas antibodies require mammalian cells for efficient production.[35]

FXIa promotes coagulation through the activation of factor IX (FIX).[37] Thus, specific inhibition of FXIa activity could be achieved by targeting the FXIa–FIX interaction. The FIX binding site on FXI has been localized to the apple 3 domain using chimeric FXIa in which individual apple domains were substituted by the corresponding domain from prekallikrein.[38] FXI chimeras were able to activate FIX, with the exception of the apple 3-substituted chimera. This was supported by inhibition of FIX activation by anti-apple 3 antibodies.[38] Further mapping of the binding site localized it to amino acids Ile183, Arg184, and Asp185.[39,40]

Here we report the generation and characterization of six anti-FXI nanobodies that target the FXI apple 3 domain. Whereas five of these show inhibitory properties toward the interaction of FXI(a) with FIX, one anti-apple 3 nanobody was able to inhibit the FXI–high molecular weight kininogen (HK) interaction further elucidating the binding orientation of HK on FXI. Moreover, all nanobodies might serve as a starting point in the development of novel safe antithrombotic treatment.

Essentials

- Factor XI (FXI) is a promising target for new anticoagulant therapy.
- A panel of nanobodies targeting apple 3 domain in FXI was generated.
- Six nanobodies showed inhibition of FXI in a variety of assays.
- A unique nanobody exposes a new interaction site of high molecular weight kininogen on FXI.

---

2 | MATERIALS AND METHODS

2.1 | Materials

QuikChange and polyclonal horseradish peroxidase (HRP)-linked goat anti-mouse immunoglobulins were from Agilent. HEK293 cells were from ATCC. Cell culture media used were DMEM/F12 (Lonza) and Opti-MEM I reduced serum medium with Glutamax supplement (Gibco; Thermo Fisher Scientific). Cell Factories and TripleFlasks were obtained from Thermo Fisher Scientific. Geneticin (G-418 sulfate) was from Calbiochem (Merck). Peptide-IV (HSDDDWIPDIQT DPNGLSFNPISDFPDTTSPK-OH)[41] was provided by Thermo Fisher Scientific and coupled to CNBr-Activated Sepharose 4 Fast Flow (GE Healthcare Life Sciences). A Fresenius polysulfone low-flux dialyser F5HPS (Fresenius Medical Care) was used as an artificial kidney. Diisopropyl fluorophosphate (DFP) and polyethylene glycol (PEG) 6000 were purchased from Sigma-Aldrich. Deep-well plates were from Thermo Fisher Scientific. Permeable membranes were obtained from Diversified Biotech. Anti-myc antibody (9E10) and primers M13R and M13F were from Invitrogen. DNAseI was from Affymetrix, and PD10 columns from GE Healthcare. Amicon Ultra4 centrifugal filter (10 kDa MWCO) were from Millipore (Merck). The surface plasmon resonance CM5 sensor chip and amine-coupling kit were from Cytiva. Chromogenic substrate S2366 was obtained from

Chromogenix. HK, FXIIa, and corn trypsin inhibitor (CTI) were from Enzyme Research Laboratories. Deuterium oxide 99.9% and CaCl$_2$ 1 M solution were from Sigma-Aldrich. Tris (2-carboxyethyl)phosphine hydrochloride (TCEP HCl) was from Thermo Fisher Scientific. Ultrapure Urea and 5 M NaCl solution (Molecular Biology grade) were obtained from Invitrogen. 1 M Hepes buffer was from Gibco. NaOH 10 M was from Alfa Aesar.

2.2 | Methods

2.2.1 | Cell culture, protein expression, and protein purification

Recombinant FXI cDNA with a Cys11Ser mutation[42] was introduced in pCDNA3.1. FXI-N90QN126Q was prepared from FXI wild type (WT) by Quikchange mutagenesis. Sequence analysis was used to confirm the introduced mutation. FXI-WT and FXI-N90QN126Q were stably transfected in HEK293 cells using calcium precipitation. Medium with 5% fetal calf serum was used to expand and grow cells in a Cell Factory (6320 cm^2) for expression. At confluence, serum-free medium (Optimem/Glutamax 1) was added and collected every 48–72 h. FXI was purified from expression medium using a peptide IV column[42] after concentrating the collected medium over an artificial kidney. The peptide IV column was eluted with 100 mM citrate pH 5.0, 1 M NaCl, and 10 mM ethylenediaminetetraacetic acid. The eluent was checked for contamination with FXIa with chromogenic substrate S2366. Contaminating enzymes, including FXIa, were eliminated by treatment with serine protease inhibitor DFP until chromogenic activity was inhibited. FXI-WT was dialyzed against 10 mM Hepes, pH 7.5, containing 0.5 M NaCl and stored at −80°C. FXI-N90QN126Q was dialyzed against 10 mM Hepes, pH 7.5, containing 0.15 M NaCl and stored at −80°C. The concentration of recombinant protein was determined by measuring the absorbance at 280 nm using the extinction coefficient for FXI (13.4).

2.2.2 | Activation of FXI to FXIa

FXI was incubated with FXIIa (molar ratio 20:1) in assay buffer (25 mM HEPES, 127 mM NaCl, 3.5 mM KCl, 3 mM CaCl$_2$) with 0.1% PEG6000 for 72 h at 37°C. FXIa was purified using the peptide IV column as described above.

2.2.3 | Llama immunization, bacteriophage library construction, and initial nanobody selection against FXI

Two llamas were subcutaneously injected with a mixture of FXI and FXIa, which were generated as previously described.[43] A bacteriophage library was prepared from RNA obtained from peripheral blood lymphocytes of the animals as described by de Maat et al.[44]

Nanobody selection was essentially performed as described by de Maat et al., but selection was on immobilized FXI. Sanger Sequencing was performed to select unique nanobodies.

2.2.4 | Solid-phase binding assay for selection of FXI-targeting nanobodies

Recombinant FXI (1 μg/ml) was immobilized overnight at 4°C in coating buffer (50 mM NaHCO$_3$, pH 9.6) in Nunc Maxisorp 96-well microtiter plates. Wells were blocked with block buffer (1% skimmed milk in phosphate-buffered saline [PBS], 0.1% Tween20) for 1 h at room temperature (RT). Plates were washed with washing buffer (PBS, 0.1% Tween20) and 50 μl nanobody in growth medium was added and incubated 1 h at RT. The plates were washed with washing buffer and incubated 1 h at RT with anti-myc antibody (9E10, 1:1000). After washing the plates with washing buffer, these were incubated with a secondary goat-anti-mouse-HRP antibody (1:1000) and incubated 1 h at RT. After rinsing with wash buffer, wells were colored with 100 μl TMB coloring solution, which was stopped after 5 min with 50 μl H$_2$SO$_4$ (1 M). Absorbance was measured at 450 nm on a SpectraMax (Molecular Devices).

2.2.5 | Nanobody production and purification

Nanobody production was induced in an overnight culture of infected *E. coli* TG1 in Yeast-Tryptone medium with ampicillin (100 μg/ml) and glucose (0.2% m/v) by addition of isopropyl β-D-1 thiogalactopyranoside (0.1 M final concentration). After overnight culture, nanobodies were purified with a Cobalt-NTA (Talon) column (BD Biosciences), eluted with a buffer containing 25 mM HEPES (pH 7.8), 500 mM NaCl, and 125 mM imidazole. Hereafter, the buffer was changed to HBS (10 mM HEPES, 150 mM NaCl, pH 7.4) with a PD10 column. Nanobody-containing fractions from this buffer change were combined and concentrated using an Amicon filter (MWCO 10 kDa). Concentrations were determined by measuring the OD$_{280nm}$ on a NanoDrop 1000. The following assays were performed with purified nanobodies.

2.2.6 | Chromogenic assays with FXI/FXIa

Nanobody influence on FXIa activity
FXIa (5 nM, all concentrations are given as final concentration) and nanobody (200 nM) in assay buffer (25 mM Hepes, pH 7.4, 137 mM NaCl, 3.5 mM KCl, 3 mM CaCl$_2$, 0.1% BSA), were incubated for 15 min at 37°C. Hereafter, S2366 (0.5 mM) was added and the absorbance at 405 nm was measured for 10 min at 37°C.

Activation of FIX by FXIa
The effect of nanobodies on activation of FIX by FXIa was determined using the Rossix FXIa kit according to protocol of the

manufacturer. In a microtiter well, nanobody or assay buffer was combined with FXIa (1 pM). This was incubated for 30 min at 37°C after which 25 μl reagent 1 (FIX, preheated at 37°C) was added. After 4 min incubation, 25 μl reagent 2 (FX, preheated at 37°C) was added and the mixture was incubated for an additional 2 min. After addition of 25 μl FXa substrate (preheated at 37°C), absorbance was measured at 405 nm.

2.2.7 | Plasma-based coagulation assays

Activated partial thromboplastin time, prothrombin time, and FXI activity

Coagulation factor assays prothrombin time (PT), activated partial thromboplastin time (APTT), and FXI activity were performed on an automated coagulation analyzer (Behring Coagulation System) with reagents and protocols from the manufacturer (Siemens Healthcare Diagnostics).

Thrombin generation

The Calibrated Automated Thrombogram® (CAT) assays the generation of thrombin in clotting plasma using a microtiter plate reading fluorometer (Fluoroskan Ascent, ThermoLab systems) and Thrombinoscope® software (Thrombinoscope BV). The assay was carried out as described by Hemker et al.[45] and the Thrombinoscope manual. Coagulation was triggered by recalcification of platelet-poor plasma substituted with nanobodies or a combination of monoclonal antibodies #203 and #175[46] in the presence of platelet-poor plasma low reagent (1 pM recombinant human tissue factor and 4 μM phospholipids), or diluted APTT reagent (Actin FSL, 20 times diluted in MP reagent, 4 μM phospholipids), and 417 μM fluorogenic substrate Z-Gly-Gly-Arg-AMC (Bachem). Fluorescence was monitored using the Fluoroskan Ascent fluorometer (Thermo Labsystems), and the endogenous thrombin potential was calculated using the Thrombinoscope software (Thrombinoscope BV).

2.2.8 | Surface plasmon resonance experiments

Epitope mapping of nanobodies on FXI

Surface plasmon resonance (SPR) experiments were performed on a BIACORE T200 (Cytiva, formerly GE Healthcare) equipped with a CM5 sensor chip. To determine the nanobody epitopes, the individual apple domains fused to tissue plasminogen activator,[47] FXI, FXIa, or kallikrein were immobilized on the chip (1200, 2200, 2200, or 1400 RU, respectively) using amine-coupling chemistry according to the manufacturer's protocol (GE Healthcare). Analytes (anti-FXI nanobodies or anti-FXI IgG) diluted in running buffer (10 mM Hepes, 150 mM NaCl, 0.01% surfactant P20, pH 7.5) were injected over the flow cells at a flow rate of 30 μl/min at 25°C. Complexes were allowed to associate and dissociate for 180 and 300 s, respectively. Surfaces were regenerated after each experiment with a 10 s

injection of 0.85% H_3PO_4. The sensorgram data were analyzed with the BIAevaluation software (Biacore) and with Scrubber (BioLogic Software).

Epitope binning

Nanobody epitope binning was performed by subsequent injection of two nanobodies over the FXI–apple domain of interest. Responses were measured at the end of the first nanobody injection (1), at the end of the first nanobody dissociation (2), and at the end of the second nanobody injection (3). Nanobodies were regarded as competitive when the value of 3–2 was ≥65% lower than the value at point 1.

2.2.9 | Solid-phase assay for measuring nanobody competition with HK binding to FXI

HK (0.5 μg/ml) was immobilized overnight at 4°C in coating buffer (50 mM $NaHCO_3$, pH 9.6) in Nunc Maxisorp 96-well microtiter plates. Wells were blocked with block buffer (1.5% BSA in PBS) for 1 h at RT. FXI (4 nM) was pre-incubated with the nanobodies for 1 h at RT. Plates were washed with washing buffer (PBS, 0.1% Tween20) and the pre-incubated samples were incubated 2 h at RT. The plates were washed with washing buffer and incubated 2 h at RT with polyclonal anti-FXI antibody (2 μg/ml). After washing the plates with washing buffer, these were incubated with a secondary swine-anti-rabbit-HRP antibody (0.5 μg/ml) and incubated 1 h at RT. After rinsing with wash buffer, wells were colored with 100 μl TMB coloring solution, which was stopped with 50 μl H_2SO_4 (1 M). Absorbance was measured at 450 nm on a SpectraMax (Molecular Devices).

2.2.10 | Activation of FXI by FXIIa

FXI (30 nM) and nanobody or assay buffer (25 mM Hepes, pH 7.4, 137 mM NaCl, 3.5 mM KCl, 3 mM $CaCl_2$, 0.1% ovalbumin), were incubated for 30 min at 37°C. After addition of FXIIa (5 nM) the mixture was incubated for an additional 2 h before adding CTI (25 nM). S2366 (0.5 mM) was added and the mixture was incubated for 10 min before measuring absorbance at 405 nm for 10 min at 37°C.

2.2.11 | Hydrogen–deuterium exchange mass spectrometry

Hydrogen–deuterium exchange mass spectrometry (HDX MS) was performed with the FXI-N90QN126Q mutant for increased sequence coverage of FXI. Protein samples (2 μM FXI-N90QN126Q or 2 μM FXI-N90QN126Q with 6 μM nanobody) were placed in a LEAP PAL pipetting robot (LEAP Technologies). Samples were diluted 10 times in binding buffer (10.56 mM Hepes pH 7.4, 150 mM NaCl, and 7.78 mM $CaCl_2$ in 98% D_2O), resulting in a final buffer composition

of 10.5 mM Hepes pH 7.24, 150 mM NaCl, and 7 mM $CaCl_2$. Samples were incubated for 10, 30, 100, or 300 s at 24°C. Incubation with binding buffer containing H_2O instead of D_2O was used as reference. Deuterium exchange was quenched by mixing the sample 1:1 with quenching solution (1 g TCEP-HCl dissolved in 2 ml 2 M Urea, pH 2.5) for 1 min at 4°C. The sample was digested by passing it over a Poroszyme Immobilized Pepsin cartridge with an isocratic flow of 5% acetonitrile, 0.1% formic acid for 5 min at 4°C. After collection on a trap (Acclaim Guard Column 120, C18, 5 μm, 2.0 × 10 mm), the peptides were washed for 30 s at 4°C. Subsequently, peptides were eluted and passed over a C18 column (Hypersil Gold C18: 30 mm length, 1 mm diameter, particle size 1.9 μm, Thermo cat #25002–031030) using a gradient from 0.08% to 64% acetonitrile at 50 μl/min at 4°C. Peptides were injected online into an LTQ Orbitrap XL operating in positive mode. To identify peptides and their retention times, peptides were fragmented by collision-induced dissociation (CID).

2.3 | HDX data analysis

Sequence and retention times of non-deuterated peptides were analyzed with PEAKS (version 7.0, Bioinformatics Solution Inc.). Deuterated peptides were analyzed using HDExaminer 2.2.0 (Sierra Analytics), which calculates the deuterium uptake of peptides within 1 min retention time. Identified peptides were assessed manually. Peptides were discarded if not accurately detected in at least half of the measurements for both compared samples. The percentage of deuterium uptake (%D) was calculated for each peptide relative to the theoretical maximal amount of deuterium incorporation. The presented HDX data consist of the mean value and corresponding

standard deviation of three to five independent experiments calculated individually for four different incubation times (10, 30, 100, or 300 s). Data points with a standard deviation >5% were not included. Results were visualized in a 3D protein model using PyMOL (Schrödinger).

3 | RESULTS

3.1 | Selection of FXI/FXIa binding nanobodies

Phage-display libraries were generated from peripheral blood lymphocytes obtained after immunization of two llamas with FXI and FXIa. These two libraries were panned against FXI to select for FXI-binding phages. Hereafter, the FXI-binding ability was assessed for 188 single clones per library (two rounds), selecting 76 nanobodies that showed binding in both assays. Genomic duplicates were removed from the selection. Binding of the remaining 52 nanobodies to FXI, FXIa, and kallikrein was measured using SPR. Kallikrein is a close homologue of FXI[48,49] and was included to assess the specificity of the nanobodies. Results showed that the selected nanobodies bind both FXI and FXIa, but not kallikrein (Table 1).

3.2 | Epitope mapping and binning

Because the FIX binding site is located on the FXI apple 3 domain, we selected for nanobodies that target the apple 3 domain. These nanobodies would be able to interfere sterically with the interaction between FIX and FXIa. The binding site of the FXI/FXIa-binding nanobodies was mapped to either of the four apple

TABLE 1 Association rate constants (k_a), dissociation rate constants (k_d), and affinity constants (K_D) of nanobodies for FXI, FXIa, the FXI apple 3 domain (A3), and kallikrein

	Nanobody					
Kinetics	1D4	2E3	2G3	1H9	2H5	1B3
FXI						
k_a ($M^{-1} s^{-1}$)	8.73E+04	8.70E+04	4.25E+05	3.09E+05	2.62E+05	5.94E+05
k_d (s^{-1})	5.18E-04	7.36E-04	1.11E-03	7.90E-05	7.70E-05	8.35E-05
K_D (nM)	5.9	8.5	2.6	0.3	0.3	1.4
FXIa						
k_a ($M^{-1} s^{-1}$)	8.65E+04	8.81E+04	4.35E+05	3.35E+05	2.91E+05	6.41E+04
k_d (s^{-1})	5.17E-04	7.80E-04	1.09E-03	8.33E-05	7.23E-05	7.79E-05
K_D (nM)	6	8.9	2.5	0.2	0.2	1.2
FXI-A3						
k_a ($M^{-1} s^{-1}$)	3.43E+04	3.54E+04	1.24E+05	1.09E+05	7.33E+04	4.27E+04
k_d (s^{-1})	9.78E-04	7.99E-04	9.90E-04	1.08E-04	1.14E-04	5.04E-04
K_D (nM)	28.5	22.6	8	1	1.6	11.8
Kallikrein						
K_D (nM)	NB	NB	NB	NB	NB	NB

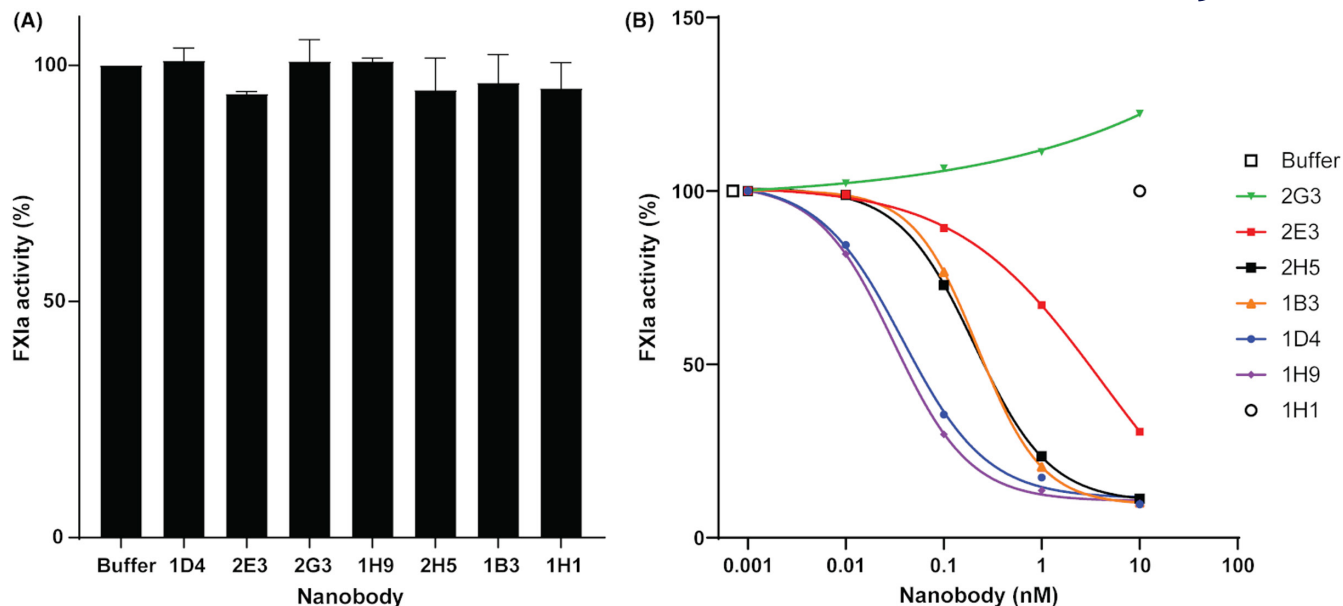Abbreviations: FXI, factor XI; FXIa, activated factor XI; NB, no binding.

FIGURE 1 Effect of nanobodies on factor XIa (FXIa) amidolytic activity and factor IX (FIX) activation by FXIa. A, Amidolytic activity of FXIa in the presence of apple 3 targeting nanobodies and a control nanobody (1H1). Data are represented as mean ± standard deviation, $n = 3$. B, In a purified system, FXIa was incubated with nanobodies before activation of FIX. The generated FIXa was analyzed with factors VIII and X by measuring factor Xa generation. □, buffer control; ○, nanobody 1H1. The data points represent the mean value of two independent experiments.
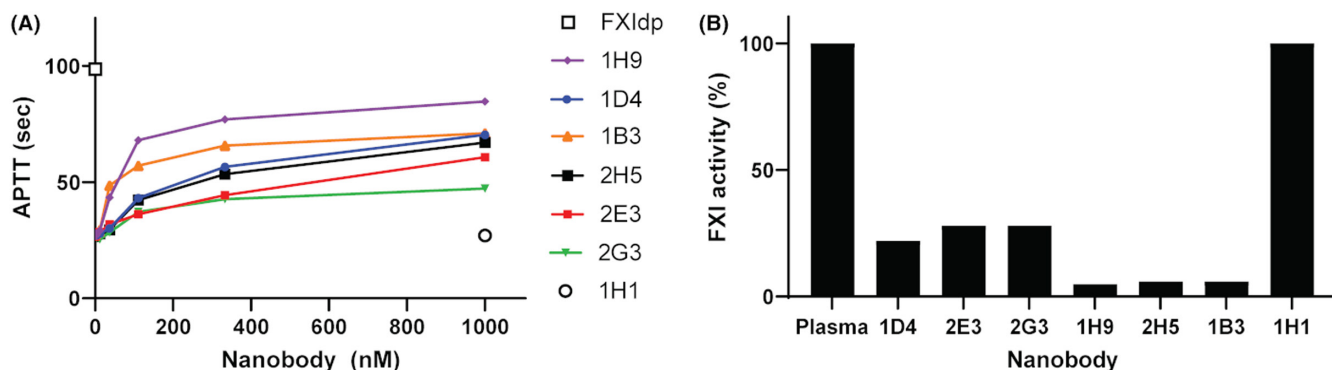

FIGURE 2 Factor XI (FXI) nanobodies affect coagulation. Normal human plasma was spiked with nanobodies at the indicated concentrations. A, Activated partial thromboplastin time (APTT) of nanobody-spiked plasma. □, FXI-depleted plasma (FXIdp); ○, nanobody 1H1. B, FXI activity determination of nanobody-spiked plasma.

domains of FXI with SPR, resulting in the identification of six apple-3 binding nanobodies to be characterized in following assays. The affinities of these nanobodies were obtained for FXI, FXIa, and the apple 3 domain (Table 1). Moreover, epitope binning was performed within the apple 3 domain. This binning indicated that all nanobodies but 2G3 share a binding epitope within the apple 3 domain (data not shown).

3.3 | Effect of nanobodies on FIX activation by FXIa

After establishing that the nanobodies did not influence FXIa's amidolytic activity (Figure 1A), the effect of these nanobodies on FIX

activation by FXIa was tested in a purified system. All nanobodies but 2G3 were able to dose-dependently inhibit FIX activation by FXIa (Figure 1B). Nanobodies 1H9 and 1D4 were the most potent and reached complete inhibition.

3.4 | APTT, PT, and FXI activity

The influence of the nanobodies on coagulation was then evaluated in plasma. As expected, the anti-FXI nanobodies did not affect the PT (data not shown). On the other hand, all nanobodies had an effect on the APTT, and FXI activity (Figure 2). All six nanobodies prolonged the clotting time in the APTT in a concentration-dependent manner (Figure 2A). The effect on FXI
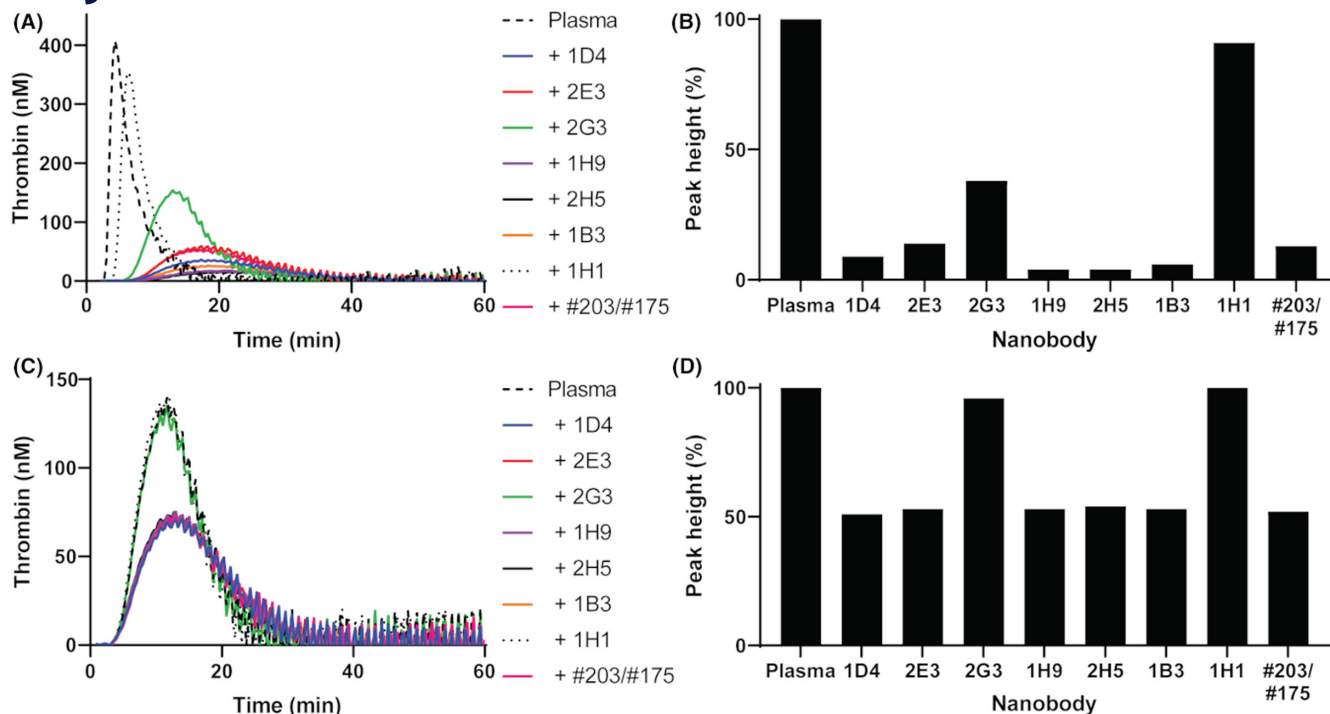
FIGURE 3 Factor XI (FXI) nanobodies affect thrombin generation initiated via the intrinsic (A,B) or extrinsic (C,D) pathway. Thrombogram obtained from thrombin generation analysis performed with the Calibrated Automated Thrombogram® (CAT) assay. Normal human plasma was spiked with nanobodies or monoclonal antibodies #203/#175 (1 μM) and activated with diluted activated partial thromboplastin time (APTT) reagent (A) or 1 pM tissue factor (C). Peak thrombin levels (B,D) were derived from (A,C) respectively.

activity was tested with 1 μM nanobody, at which most nanobodies had shown a maximal effect in the APTT. All nanobodies show more than a 50% reduction in FXI(a) activity (Figure 2B). Strikingly, 2G3 prolonged APTT and reduced FXI activity although it did not affect FIX activation by factor XIa. Of the six nanobodies only 2G3 was able to prolong the APTT in mouse plasma (data not shown).

3.5 | Thrombin generation

The anticoagulant function of the nanobodies was tested in thrombin generation analyses under both intrinsic and extrinsic coagulation conditions. All nanobodies had profound effects on both lag time (Figure 3A) and peak height (Figure 3A,B) when thrombin generation was initiated via the intrinsic pathway. Most nanobodies inhibited thrombin generation almost completely, with the exception of 2G3, which reduced thrombin generation by 50%. When thrombin generation was initiated via the extrinsic pathway with tissue factor, there was no effect on lag time (Figure 3C). The peak height was reduced by approximately 50% for all nanobodies but 2G3, which had no effect (Figure 3D). A reduction to 50% corresponds with full inhibition of FXI(a) as FXI depleted plasma (data not shown) or inhibition by monoclonal anti-FXI antibodies (#203 and #175, Figure 3) retained 50% peak thrombin levels.[46]

3.6 | Effect of nanobodies on FXI–HK interaction and activation of FXI by FXIIa

Although nanobody 2G3 did not affect the FXI–FIX interaction, it demonstrated an inhibitory effect on coagulation mediated by the intrinsic pathway. We therefore assessed whether the nanobodies influenced interaction of FXI with HK or FXIIa-mediated FXI activation. Five nanobodies left the FXI–HK interaction unaffected (Figure 4A), but impeded FXIIa-mediated activation of FXI. Conversely, 2G3 showed a strong inhibitory effect on the FXI–HK interaction but did not affect FXI activation by FXIIa (Figure 4B).

3.7 | HDX MS

To relate the two different mechanisms of action that we observed to the binding epitopes of the nanobodies, the binding site of 1H9 and 2G3 on FXI was characterized with HDX MS. Nanobody 1H9 showed the greatest effect on FXI(a) activity in the assays, while nanobody 2G3 was the only nanobody with an alternative binding epitope. In HDX MS the extent of deuterium exchange of a protein region can be related to its solvent accessibility in the protein or its structural rigidity. Thus, a reduction in deuterium uptake can be related to binding of a ligand (i.e., a nanobody) or increased rigidity induced either locally or allosterically by the interaction.[50,51] A difference greater than 6% over at least three out of four time points
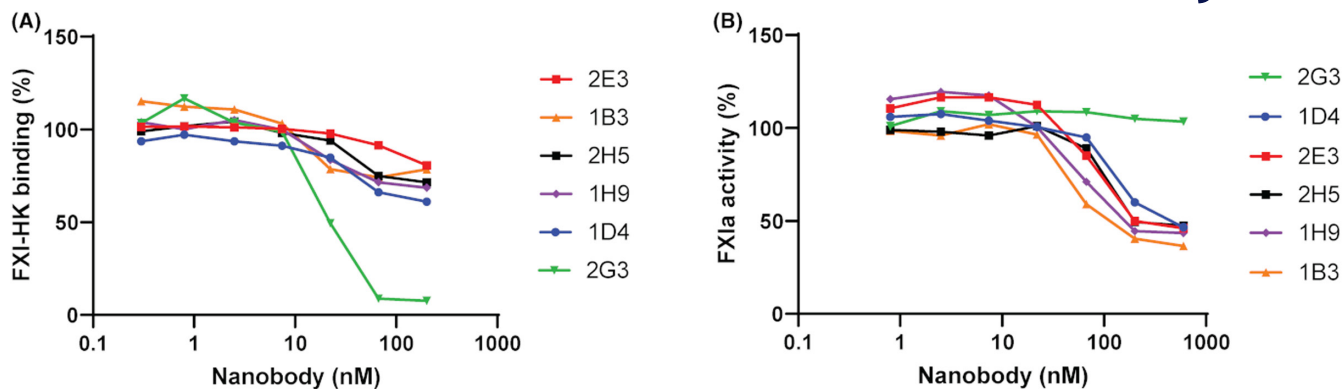
FIGURE 4 Effect of nanobodies on high molecular weight kininogen (HK) interaction with factor XI (FXI) and FXI activation by factor XIIa (FXIIa). A, Effect of nanobodies on HK interaction with FXI. FXI was incubated with increasing concentrations of nanobody before addition to HK in a solid-phase assay. B, Effect of nanobodies on FXI activation by FXIIa. In a purified system, FXI was incubated with nanobodies before activation by FXIIa. The data represent the mean value of two independent experiments.
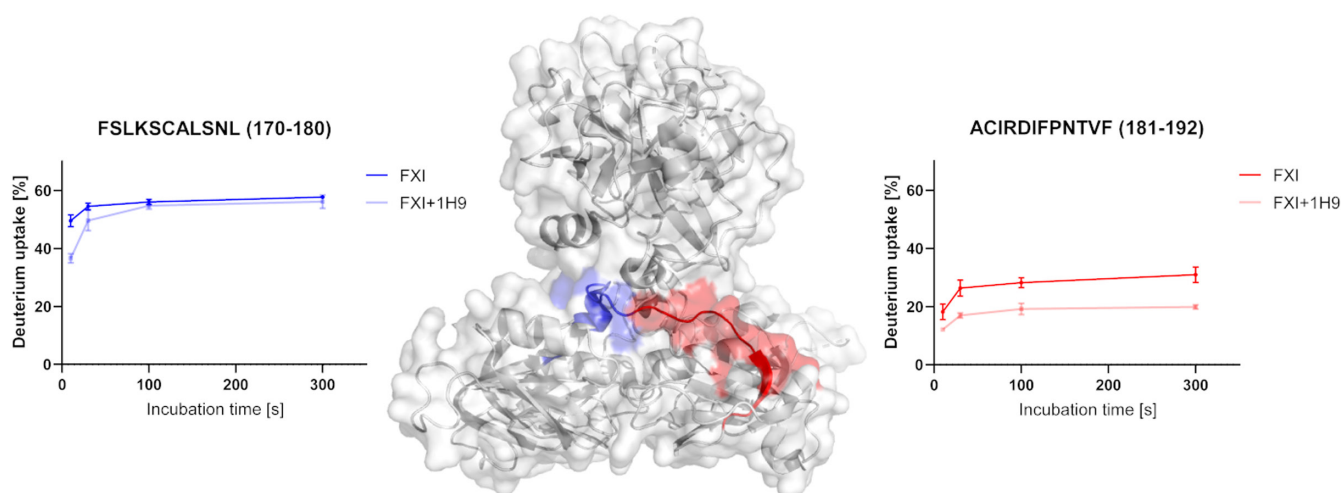

FIGURE 5 Regions in which the interaction with nanobody 1H9 induced a reduction in deuterium uptake highlighted in the crystal structure of factor XI (FXI; PDB 6i58).[52] The main region affected by the FXI–1H9 interaction consists of the beginning of the apple 3 domain up until the first beta-strand (Ala181-Phe192, red). Moreover, the region connecting the apple 2 and apple 3 domain (Phe170-Leu180, blue) shows a small reduction in deuterium uptake at 10 s.

for one peptide was regarded as induced by binding, as long as this was consistent for overlapping peptides. Additionally, consistent differences in deuterium uptake of at least 6% for at least one time point over multiple overlapping peptides within one peptide region were considered to result from the interaction. These differences could result either from binding interactions or from induction of allosteric rigidity. The deuterium uptake plots of the complete set of peptides detected in FXI in the presence of nanobodies are included in Figure S1 in supporting information.

Interaction of nanobody 1H9 with FXI affected two adjacent peptide regions: Phe^{170}-Leu^{180} and Ala^{181}-Phe^{192}. The latter, located at the beginning of the apple 3 domain (red, Figure 5), shows a marked reduction in deuterium uptake over all four time points. It is therefore proposed to be the main binding site of the nanobody. The former region, which consists of the end of the loop connecting the apple 2 to the apple 3 domain (blue, Figure 5), shows a consistent decrease in deuterium uptake at 10 s incubation over multiple

overlapping peptides, which could point to a transient effect induced by binding.

Nanobody 2G3 shows a strong reduction of deuterium uptake for regions Ala^{193}-Ala^{205} and Leu^{239}-Phe^{260} (red, Figure 6A,B). Moreover, a smaller but consistent effect is observed for Phe^{224}-Leu^{238} (blue, Figure 6B). Additionally, multiple regions in FXI show transient reduction of the deuterium uptake as a result of the introduction of 2G3. These include Ser^{63}-Gly^{79} in the apple 1 domain, Phe^{170}-Leu^{180} in the loop connecting the apple 2 and apple 3 domain, and Trp^{497}-Glu^{525} in the catalytic domain (green, Figure 6B).

4 | DISCUSSION

The clinical potential of FXI as a target for new anticoagulant therapies with a reduced bleeding risk has been reinforced by the emergence of various therapeutic agents, such as antibodies,
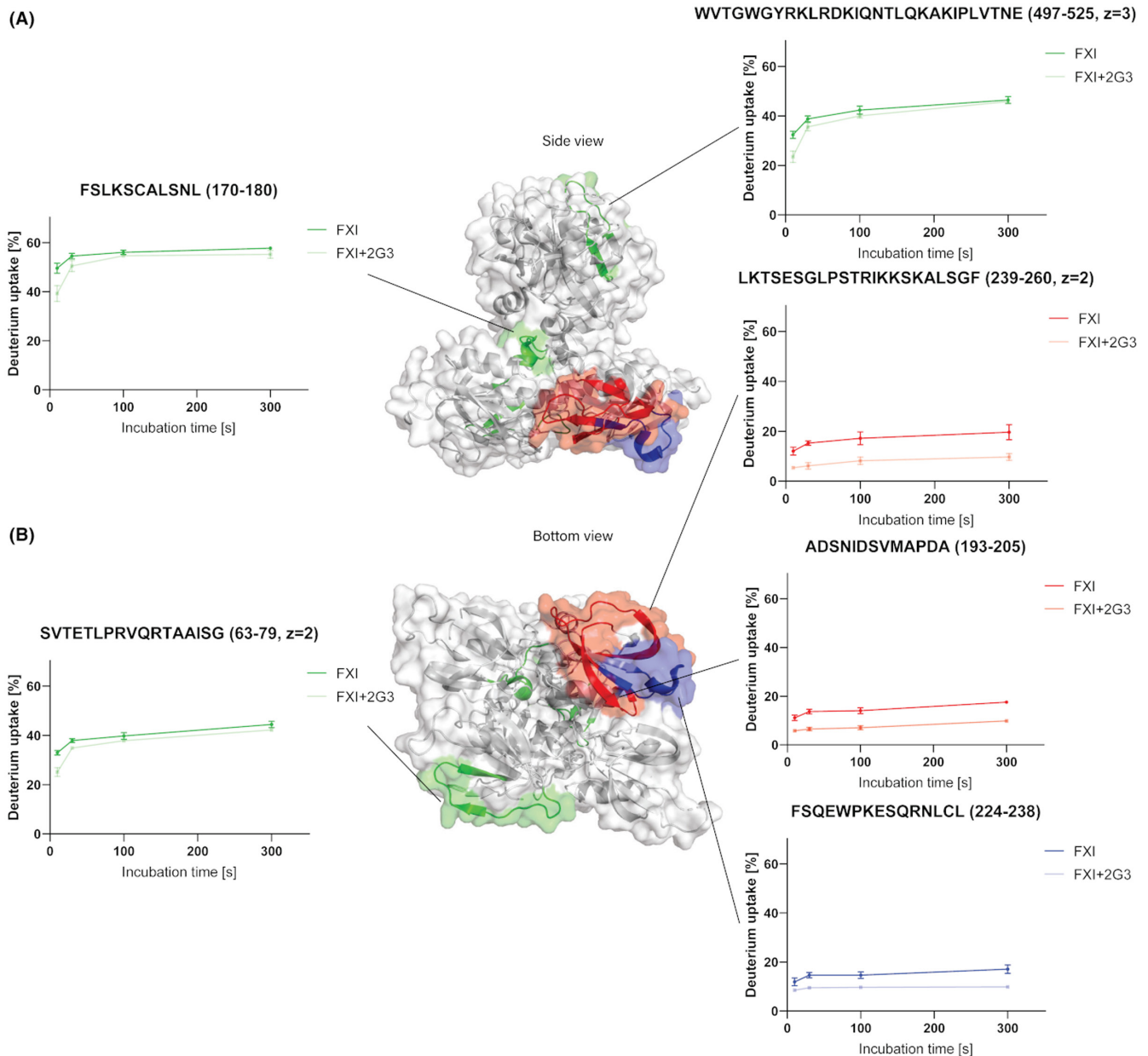
(A)

FSLKSCALSNL (170-180)

WVTGWGYRKLRDKIQNTLQKAKIPLVTNE (497-525, z=3)

Side view

(B)

Bottom view

SVTETLPRVQRTAAISG (63-79, z=2)

LKTSESGLPSTRIKKSKALSGF (239-260, z=2)

ADSNIDSVMAPDA (193-205)

FSQEWPKESQRNLCL (224-238)

FIGURE 6 Side (A) and bottom (B) view of factor XI (FXI) crystal structure (PDB 6i58)[52] in which regions affected by the FXI–2G3 interaction have been highlighted. Introduction of 2G3 had a great effect on the deuterium uptake of the beta-sheet in the apple 3 domain (Ala193-Ala205 and Leu239-Phe260, red) as well as a smaller effect on a connecting loop on the outside of the apple 3 domain (Phe224-Leu238, blue). Additionally, multiple short-lived reductions in deuterium uptake were observed in the apple 1 domain, in the loop connecting the apple 2 domain to the apple 3 domain, and in the catalytic domain (green).

targeting FXI that have reached clinical trials.[2,23–25,53] Nevertheless, the development of novel anticoagulants remains relevant as repeated administration of biopharmaceuticals has been related to the development of adverse immunogenicity against treatment with effects ranging from reduced bioavailability to the instigation of an autoimmune response.[28,29] Therefore, we have focused on the generation of FXI-targeting nanobodies. Nanobodies have a comparable target specificity to antibodies, but are known to be less immunogenic.[30,35] Additionally, nanobodies show high solubility, efficient tissue penetration, and can be more readily produced in bacteria or yeast.[29–31,34,35] We focused on nanobodies targeting the apple 3

domain as it mediates the interaction between FXIa with its ligand FIX.[38,40]

In this study, we report the generation of six nanobodies targeting the FXI apple 3 domain that were able to attenuate coagulation to varying degrees. The nanobodies showed binding to FXI and FXIa but not to their homologue kallikrein. This suggests that the nanobodies are highly selective for FXI/FXIa, limiting the chances of off-target effects in further nanobody development. Five of the anti-apple 3 nanobodies were able to inhibit the activation of FIX by FXIa, suggesting direct competition with FIX as its binding site on FXI is also located on the apple 3 domain.[39,40,43]
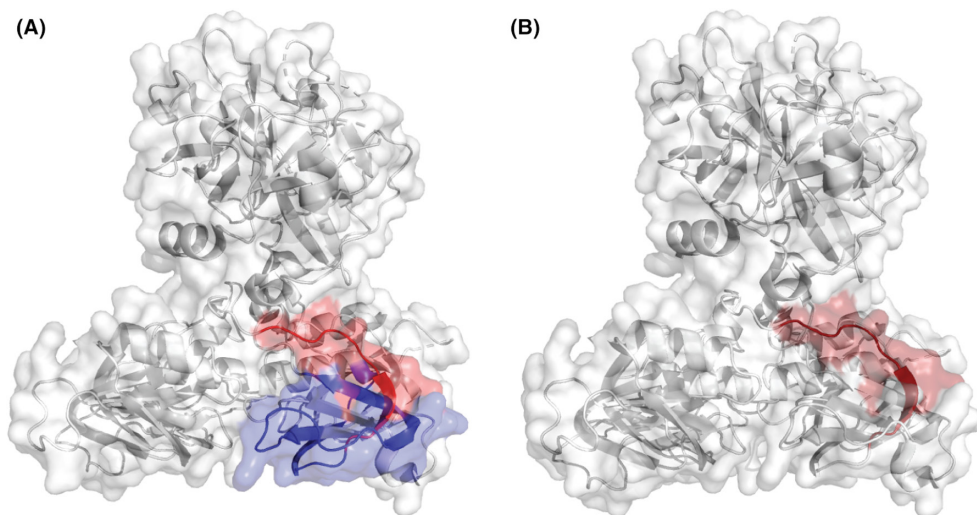
FIGURE 7 Main binding epitopes of (A) 1H9 (red), 2G3 (blue), or (B) factor IX (FIX; dark red) plotted into crystal structure of FXI (PDB 6i58).[52]

Subsequent epitope binning illustrated that these five nanobodies have an overlapping binding site, while 2G3, which does not compete with the FXIa–FIX interaction, has a unique binding epitope. Alternately, 2G3 is the only nanobody that affects the FXI–HK binding.

To characterize the two identified binding epitopes, HDX MS was performed for 1H9, which had the highest potency, and 2G3. This analysis demonstrated great overlap between the binding epitope of 1H9 and the previously reported binding region of FIX on FXIa as identified with mutation studies as well as HDX MS (Figure 7).[39,40,43] This further supports the hypothesis that observed effects on coagulation result from direct competition of the nanobody with FIX. While this binding site seems accessible for 1H9 in both FXI and FXIa, the binding site is masked for FIX in FXI and only becomes available for binding after rotation of the catalytic domain upon conversion to FXIa.[43,54]

Furthermore, HDX MS confirmed a different binding epitope on FXI for 2G3, located at the bottom of the apple 3 domain. A reduction in deuterium uptake was most evident for the peptides spanning the second, fourth, and fifth beta strand of the apple domain (Ala^{193}-Ala^{205} and Leu^{239}-Phe^{260}). We thus propose this to be the main binding site for the nanobody. Additionally, a smaller effect was observed for the loop connecting the third and fourth beta strand (Phe^{224}-Leu^{238}) that is located in the same plane as the main binding region. This could either result from 2G3 binding to this loop, or indirectly by 2G3 increasing the loop's rigidity.

Characterization of 2G3's binding epitope on FXI clarifies why it does not interfere with FIX activation by FXIa. 2G3 interacts with the bottom plane of the apple 3 domain, whereas FIX binding occurs on the top of the apple 3 domain (Figure 7).[39,40,43] Moreover, 2G3 further elucidates the binding orientation of HK on FXI. This interaction had been localized to the apple 2 domain.[55] The competition with 2G3 suggests that HK binding extends toward the apple 3 domain. This competition with HK illustrates how 2G3 is able to affect coagulation in plasma-based coagulation assays (APTT, FXI activity, and the intrinsic CAT). HK is required for localization of FXI to surfaces for subsequent activation of FXI by FXIIa.[56,57] Inhibition of the FXI–HK interaction will therefore indirectly lead to impaired coagulation.[58]

Besides the main binding site in the apple 3 domain, 2G3 induces transient effects in various other regions. These effects were observed in the outer beta strand of the apple 1 domain (Ser^{63}-Gly^{79}), the loop connecting the apple 2 to the apple 3 domain (Phe^{170}-Ala^{176}), and the 148-loop in the catalytic domain (Trp^{497}-Glu^{525}). Reduction of the deuterium uptake suggests that these regions become more rigid as a result of nanobody binding, but these effects need further characterization to be understood.

HDX MS could not provide an explanation for the inhibitory effect of the nanobodies on FXIIa-mediated FXI activation. Direct competition seems unlikely because the nanobodies bind the apple 3 domain while previously reported binding sites for FXIIa include the apple 2 or apple 4 domain.[58,59] The apple 3-targeting nanobodies might exert steric hindrance on FXIIa binding to an adjacent apple domain. FXIIa may also partake in interactions with the apple 3 domain to support a main binding on a different apple domain. It remains important to better characterize the FXIIa binding site on FXI.

In conclusion, we hereby present six nanobodies that could serve as interesting tool compounds in further research on FXI. These nanobodies could serve as lead compounds in the development of novel antithrombotic therapy, and translation to animal models is required. Nanobody 2G3 cross-reacts with mouse FXI and can be used directly in thrombotic models in mice. The other nanobodies could be tested in FXI-deficient mice supplemented with human FXI.[46] Five of the nanobodies function by sterically inhibiting the FIX–FXIa interaction, while one, 2G3, competes with HK binding to FXI. Interestingly, characterization of the binding epitope of 2G3, which has a unique binding epitope on the apple 3 domain, provides new insights into the binding orientation of HK when bound to FXI.

AUTHOR CONTRIBUTIONS

JCMM designed and supervised the study. ABB, JAM, and KB performed experiments and analyzed data. ABM and RTU supervised mass spectrometry analysis and nanobody generation, respectively. ABB and JCMM wrote the manuscript with input from all authors. All authors approved the final manuscript.

FUNDING INFORMATION

ORCID

Awital Bar Barroeta https://orcid.org/0000-0002-0744-5569

J. Arnoud Marquart https://orcid.org/0000-0002-2713-6165

Kamran Bakhtiari https://orcid.org/0000-0002-7818-7966

Alexander B. Meijer https://orcid.org/0000-0002-5447-7838

Rolf T. Urbanus https://orcid.org/0000-0002-1601-9393

Joost C. M. Meijers https://orcid.org/0000-0002-4198-6780

REFERENCES

1. Gailani D, Bane CE, Gruber A. Factor XI and contact activation as targets for antithrombotic therapy. *J Thromb Haemost*. 2015;13:1383-1395.
2. Weitz JI, Fredenburgh JC. Factors XI and XII as targets for new anticoagulants. *Front Med*. 2017;4:1-6.
3. Gailani D. Future prospects for contact factors as therapeutic targets. *Hematology Am Soc Hematol Educ Program*. 2014;1:52-59.
4. Gailani D, Gruber A. Factor XI as a therapeutic target. *Arterioscler Thromb Vasc Biol*. 2016;36:1316-1322.
5. Löwenberg EC, Meijers JCM, Monia BP, Levi M. Coagulation factor XI as a novel target for antithrombotic treatment. *J Thromb Haemost*. 2010;8:2349-2357.
6. Connors JM. Testing and monitoring direct oral anticoagulants. *Blood*. 2018;132:2009-2015.
7. Hellenbart EL, Faulkenberg KD, Finks SW. Evaluation of bleeding in patients receiving direct oral anticoagulants. *Vasc Health Risk Manag*. 2017;13:325-342.
8. Ruff CT, Giugliano RP, Braunwald E, et al. Comparison of the efficacy and safety of new oral anticoagulants with warfarin in patients with atrial fibrillation: a meta-analysis of randomised trials. *Lancet*. 2014;383:955-962.
9. Chan NC, Paikin JS, Hirsh J, Lauw MN, Eikelboom JW, Ginsberg JS. New oral anticoagulants for stroke prevention in atrial fibrillation: impact of study design, double counting and unexpected findings on interpretation of study results and conclusions. *Thromb Haemost*. 2014;111:798-807.
10. James P, Salomon O, Mikovic D, Peyvandi F. Rare bleeding disorders - bleeding assessment tools, laboratory aspects and phenotype and therapy of FXI deficiency. *Haemophilia*. 2014;20:71-75.
11. Ratnoff OD, Colopy JE. A familial hemorrhagic trait associated with a deficiency of a clot-promoting fraction of plasma. *J Clin Invest*. 1955;34:602-613.
12. Preis M, Hirsch J, Kotler A, et al. Factor XI deficiency is associated with lower risk for cardiovascular and venous thromboembolism events. *Blood*. 2017;129:1210-1215.
13. Renné T, Oschatz C, Seifert S, et al. Factor XI deficiency in animal models. *J Thromb Haemost*. 2009;7:79-83.
14. Salomon O, Steinberg DM, Koren-Morag N, Tanne D, Seligsohn U. Reduced incidence of ischemic stroke in patients with severe factor XI deficiency. *Blood*. 2008;111:4113-4117.
15. Meijers JCM, Tekelenburg WLH, Bouma BN, Bertina RM, Rosendaal FR. High levels of coagulation factor XI as a risk factor for venous thrombosis. *N Engl J Med*. 2000;342:696-701.
16. Yang DT, Flanders MM, Kim H, Rodgers GM. Elevated factor XI activity levels are associated with an increased odds ratio for cerebrovascular events. *Am J Clin Pathol*. 2006;126:411-415.
17. Zhang H, Löwenberg EC, Crosby JR, et al. Inhibition of the intrinsic coagulation pathway factor XI by antisense oligonucleotides: a novel antithrombotic strategy with lowered bleeding risk. *Blood*. 2010;116:4684-4692.
18. Yau JW, Liao P, Fredenburgh JC, et al. Selective depletion of factor XI or factor XII with antisense oligonucleotides attenuates catheter thrombosis in rabbits. *Blood*. 2014;123:2102-2107.
19. Al-Horani RA, Abdelfadiel EI, Afosah DK, et al. A synthetic heparin mimetic that allosterically inhibits factor XIa and reduces thrombosis in vivo without enhanced risk of bleeding. *J Thromb Haemost*. 2019;17:2110-2122.
20. Al-horani RA, Desai UR. Factor XIa inhibitors: a review of patent literature. *Expert Opin Ther Pat*. 2016;26:323-345.
21. Woodruff RS, Ivanov I, Verhamme IM, Gailani D, Sullenger BA. Generation and characterization of aptamers targeting factor XIa. *Thromb Res*. 2017;156:134-141.
22. Tucker EI, Marzec UM, White TC, et al. Prevention of vascular graft occlusion and thrombus-associated thrombin generation by inhibition of factor XI. *Thromb Haemost*. 2009;113:936-944.
23. Lorentz CU, Verbout NG, Wallisch M, et al. Contact activation inhibitor and factor XI antibody, AB023, produces safe, dose-dependent anticoagulation in a phase 1 first-in-human trial. *Arterioscler Thromb Vasc Biol*. 2019;39:799-809.
24. Koch AW, Schiering N, Melkko S, et al. MAA868—a novel FXI antibody with a unique binding mode—shows durable effects on markers of anticoagulation in humans. *Blood*. 2019;133(13):1507-1516.
25. Thomas D, Thelen K, Kraff S, et al. BAY 1213790, a fully human IgG1 antibody targeting coagulation factor XIa: first evaluation of safety, pharmacodynamics, and pharmacokinetics. *Res Pract Thromb Haemost*. 2019;3(2):242-253.
26. Verhamme P, Yi BA, Segers A, et al. Abelacimab for prevention of venous thromboembolism. *N Engl J Med*. 2021;385:609-617.
27. Beavers CJ, Wayne NB. Osocimab: a novel agent in preventing venous thromboembolism. *J Cardiovasc Pharmacol*. 2020;76:645-649.
28. Tovey MG, Lallemand C. Immunogenicity and other problems associated with the use of biopharmaceuticals. *Ther Adv Drug Saf*. 2011;2:113-128.
29. Buelens K, Hassanzadeh-Ghassabeh G, Muyldermans S, Gils A, Declerck PJ. Generation and characterization of inhibitory nanobodies towards thrombin activatable fibrinolysis inhibitor. *J Thromb Haemost*. 2010;8:1302-1312.
30. Loris R, Saerens D, Martinez-rodriguez S, Muyldermans S. General strategy to humanize a camelid single-domain antibody and identification of a universal humanized nanobody scaffold. *J Biol Chem*. 2009;284:3273-3284.
31. Wesolowski J, Alzogaray V, Reyelt J, et al. Single domain antibodies: promising experimental and therapeutic tools in infection and immunity. *Med Microbiol Immunol*. 2009;198:157-174.
32. Mitchell LS, Colwell LJ. Comparative analysis of nanobody sequence and structure data. *Proteins*. 2018;86:697-706.
33. Chanier T, Chames P. Nanobody engineering: toward next generation immunotherapies and immunoimaging of cancer. *Antibodies*. 2019;8(1):13.
34. Bannas P, Hambach J, Koch-Nolte F. Nanobodies and nanobody-based human heavy chain antibodies as antitumor therapeutics. *Front Immunol*. 2017;8:1603.
35. Harmsen MM, De Haard HJ. Properties, production, and applications of camelid single-domain antibody fragments. *Appl Microbiol Biotechnol*. 2007;77:13-22.

36. Van Roy M, Ververken C, Beirnaert E, et al. The preclinical pharmacology of the high affinity anti-IL-6R nanobody® ALX-0061 supports its clinical development in rheumatoid arthritis. *Arthritis Res Ther.* 2015;17(1):1-6.

37. Geng Y, Verhamme IM, Messer A, et al. A sequential mechanism for exosite-mediated factor IX activation by factor XIa. *J Biol Chem.* 2012;287:38200-38209.

38. Sun Y, Gailani D. Identification of a factor IX binding site on the third apple domain of activated factor XI. *J Biol Chem.* 1996;271:29023-29028.

39. Geng Y, Verhamme IM, Sun MF, Bajaj SP, Emsley J, Gailani D. Analysis of the factor XI variant Arg184Gly suggests a structural basis for factor IX binding to factor XIa. *J Thromb Haemost.* 2013;11:1374-1384.

40. Sun MF, Zhao M, Gailani D. Identification of amino acids in the factor XI apple 3 domain required for activation of factor IX. *J Biol Chem.* 1999;274:36373-36378.

41. Naito K, Fujikawa K. Activation of human blood coagulation factor XI independent of factor XII. *J Biol Chem.* 1991;266:7353-7358.

42. Stroo I, Marquart JA, Meijers JCM, Bakhtiari K, Meijer AB. Chemical Footprinting reveals conformational changes following activation of factor XI. *Thromb Haemost.* 2018;118:340-350.

43. Bar Barroeta A, Van Galen J, Stroo I, Marquart JA, Meijer AB, Meijers JCM. Hydrogen – deuterium exchange mass spectrometry highlights conformational changes induced by factor XI activation and binding of factor IX to factor XIa. *J Thromb Haemost.* 2019;17:2047-2055.

44. De Maat S, Van Dooremalen S, De Groot PG, Maas C. A nanobody-based method for tracking factor XII activation in plasma. *Thromb Haemost.* 2013;110:458-468.

45. Hemker HC, Giesen P, Al Dieri R, et al. Calibrated automated thrombin generation measurement in clotting plasma. *Pathophysiol Haemost Thromb.* 2003;33:4-15.

46. van Montfoort ML, Knaup VL, Marquart JA, et al. Two novel inhibitory anti-human factor XI antibodies prevent cessation of blood flow in a murine venous thrombosis model. *Thromb Haemost.* 2013;110:1065-1073.

47. Meijers J, Mulvihill E, Davie E, Chung D. Apple four in human blood coagulation factor XI mediates dimer formation. *Biochemistry.* 1992;31:4680-4684.

48. Fujikawa K, Chung D, Hendrickson L, Davie E. Amino acid sequence of human factor XI, a blood coagulation factor with four tandem repeats that are highly homologous with plasma prekallikrein. *Biochemistry.* 1986;25:2417-2424.

49. Ponczek MB, Shamanaev A, LaPlace A, et al. The evolution of factor XI and the kallikrein-kinin system. *Blood Adv.* 2020;4:6135-6147.

50. Konermann L, Pan J, Liu YH. Hydrogen exchange mass spectrometry for studying protein structure and dynamics. *Chem Soc Rev.* 2011;40:1224-1234.

51. Marcsisin SR, Engen JR. Hydrogen exchange mass spectrometry: what is it and what can it tell us? *Anal Bioanal Chem.* 2010;397:967-972.

52. Li C, Voos KM, Pathak M, et al. Plasma kallikrein structure reveals apple domain disc rotated conformation compared to factor XI. *J Thromb Haemost.* 2019;17:759-770.

53. Willmann S, Marostica E, Snelder N, et al. PK/PD modeling of FXI antisense oligonucleotides to bridge the dose-FXI activity relation from healthy volunteers to end-stage renal disease patients. *CPT Pharmacometrics Syst Pharmacol.* 2021;10:890-901.

54. Gailani D, Emsley J. Toward a better understanding of factor XI activation. *J Thromb Haemost.* 2019;17:2016-2018.

55. Renné T, Sugiyama A, Gailani D, Jahnen-dechent W, Walter U, Müller-Esterl W. Fine mapping of the H-kininogen binding site in plasma prekallikrein apple domain 2. *Int Immunopharmacol.* 2002;2:1867-1873.

56. Ivanov I, Shakhawat R, Sun M, et al. Nucleic acids as cofactors for factor XI and Prekallikrein activation: different roles for high molecular weight kininogen. *Thromb Haemost.* 2017;117:671-681.

57. Mohammed B, Matafonov A, Ivanov I, et al. An update on FXI structure and function. *Thromb Res.* 2018;161:94-105.

58. Cheng Q, Tucker EI, Pine MS, et al. A role for factor XIIa – mediated factor XI activation in thrombus formation in vivo. *Blood.* 2010;116:3981-3989.

59. Baglia FA, Jameson BA, Walsh PN. Identification and characterization of a binding site for factor XIIa in the apple 4 domain of coagulation factor XI. *J Biol Chem.* 1993;268:3838-3844.

SUPPORTING INFORMATION

Additional supporting information can be found online in the Supporting Information section at the end of this article.